Inorg. Chem. **1980**, *19*, 1652-1656

Contribution from the Departments of Chemistry, University of Southern Mississippi, Hattiesburg, Mississippi 39401,
and Henderson State University, Arkadelphia, Arkansas 71923

Coordination of Fe^{3+} in Concentrated Aqueous Solutions with Chloride Ligands

DAVID L. WERTZ* and MARCUS L. STEELE

Received August 13, 1979

X-ray diffraction measurements indicate that the solute species formed in concentrated aqueous solutions of $FeCl_3{\cdot}6H_2O$ (ICHH) and $FeCl_3$ (AIC) are different shortly after solution preparation, suggesting a slow equilibration of the solute species in one (or both) set(s) of the aqueous solutions. Octahedrally coordinated hexaaquoiron(III) and ion-pair Fe···Cl interactions account for the solute species found in the ICHH solutions. The average Fe–O distance is 2.04 ± 0.02 Å, and the ion-pair Fe···Cl distance is ca. 4.1 Å. In the concentrated AIC solutions, Fe^{3+} is tetrahedrally coordinated, and chloro bridging occurs. The Fe–Cl distance is 2.28 ± 0.02 Å and the nearest-neighbor Cl···Cl atom-pair interactions occur at ca. 3.7 Å.

Introduction

Aqueous solutions of Fe^{3+} salts have been investigated for many years. For anions which are poor coordinating ligands, i.e., ClO_4^- or NO_3^-, hexaaquoiron(III) has been proposed to be the principal solute species.[1,2] When the anion is chloride,[3-7] the solute species is reported to be more complicated, and both tetrahedrally[4] and octahedrally[5-7] coordinated Fe^{3+} complexes have been proposed. Disagreement also exists as to the identity of the nearest-neighbor ligands of Fe^{3+} and the extent of solute association in these solutions.

When anhydrous $FeCl_3$ is dissolved into a poorly coordinating solvent,[3,8] Fe^{3+} has been found to have four chloride (and no solvent) nearest neighbors. Tetrachloroferrate(III) has been reported when excess chloride is present in concentrated solutions.[4,6-10]

In an attempt to better understand the coordination features of Fe^{3+} in aqueous solutions of iron(III) chloride, we have examined two sets of stoichoimetrically equivalent solutions—one of each set prepared from anhydrous iron(III) chloride and one prepared from iron(III) chloride hexahydrate—by XRD methods.

Experimental Section

Solution Preparation. Each solution was prepared by weight from reagent grade solute and distilled deionized water. The density of each solution was measured with a density bulb. Solution parameters are shown in Table I.

Ideal Peak Calculations. The ideal peak (IP) and the ideal peak area (IPA)[11] for each of the possible Fe–ligand atom pairs were calculated from the X-ray scattering factors[12] by methods outlined in our previous papers.[13-16] The ideal peak areas calculated for one Fe–O and for one Fe–Cl atom pair are 403 e^2 and 967 e^2, respectively, for each solution.

X-ray Diffraction Methods. Approximately 1 week after solution preparation, each solution was sealed into a polyethylene sample holder which was then mounted into our X-ray diffractometer.[16] Mo Kα radiation was used in collecting data for a scattering pattern over the angular range from $\theta = 1.00°$ to $\theta = 60.00°$, or $s = 0.31$ Å^{-1} to $s = 15.34$ Å^{-1}, where $s = 4\pi\lambda^{-1}\sin\theta$, at increments in θ of 0.20°. Five scans of the entire angular range were made for each solution. Sufficient counts were obtained at each angular setting so that the relative standard deviation was $\leq 0.5\%$.[17]

The scattering data were corrected for background,[18] polarization,[19] absorption,[20] multiple scattering,[21] and incoherent scattering[22] and were fitted to $\sum\chi_i f_i^2(s)$ by methods previously described.[16] The resultant interference curve calculated for each solution (Figure 1) was transformed to obtain an atomic radial-distribution function (ARDF) for each solution by

$$D(r) = 4\pi r^2\rho_0 + (2r/\pi)\int s[i(s)][M(s)]\sin sr\,ds \qquad (1)$$

between the limits of $s = 0.00$ Å^{-1} and $s = 15.00$ Å^{-1} (Figure 2 and Table II). In this equation ρ_0 is the bulk density of the solution and $M(s) = (\sum\chi_i f_i(0)/\sum\chi_i f_i(s))^2\exp(-bs^2)$. $D(r) \simeq \sum\chi_i n_{ij}\sigma_{ij}K_{ij}\rho_{ij}(r)$, where χ_i is the mole fraction of atom i, n_{ij} is the number of ij atom pairs per atom i, σ_{ij} is a statistical counting factor (1 if i = j and 2 if i ≠ j), K_{ij} is the scattering power product for the ij atom pair, and $\rho_{ij}(r)$ represents various atom-pair distributions in the solution. Each ARDF is also presented as the pair correlation, where $g(r) = D(r)/4\pi r^2\rho_0$ (Table II).

Table I. Solution Parameters

designation	molality, m	ρ, g/mL	mole fractions Fe	Cl	O	H
A. Solutions Prepared from $FeCl_3{\cdot}6H_2O$ (ICHH)						
ICHH-1	10.4	1.349	0.0263	0.0789	0.2983	0.5965
ICHH-2	14.7	1.376	0.0300	0.0900	0.2933	0.5867
B. Solutions Prepared from $FeCl_3$ (AIC)						
AIC-1	4.9	1.485	0.0263	0.0789	0.2983	0.5965
AIC-2	5.7	1.622	0.0300	0.0900	0.2933	0.5867

Uncertainty in the ARDF. The uncertainty in $D(r)$ has been directly calculated from the XRD count data by the method of Konnert and Karle;[23] 2σ represents the uncertainty in each r value at the 95% confidence level.

---

*To whom correspondence should be addressed at the University of Southern Mississippi.

(1) M. Magini and R. Caminiti, *J. Inorg. Nucl. Chem.*, **39**, 91 (1977).
(2) M. Magini, *J. Inorg. Nucl. Chem.*, **40**, 43 (1978).
(3) D. L. Wertz and R. F. Kruh, *J. Chem. Phys.*, **50**, 4013 (1969).
(4) C. L. Standley and R. F. Kruh, *J. Chem. Phys.*, **34**, 1450 (1961).
(5) G. W. Brady, *J. Chem. Phys.*, **34**, 1450 (1961).
(6) G. W. Brady, M. B. Robin, and J. Varimbi, *Inorg. Chem.*, **3**, 1168 (1964).
(7) S. K. Sharma et al., *J. Inorg. Nucl. Chem.*, **37**, 2417 (1975); **35**, 3871 (1973).
(8) L. A. Woodward and M. J. Taylor, *J. Chem. Soc.*, 4473 (1960).
(9) J. B. Swanson and V. W. Laurie, *J. Phys. Chem.*, **69**, 244 (1965).
(10) H. Freedman, *J. Am. Chem. Soc.*, **74**, 5 (1952).
(11) J. Waser and V. Schomaker, *Rev. Mod. Phys.*, **25**, 671 (1953).
(12) F. Hajdu, *Acta Crystallogr. Sect. A*, **28** 250 (1972).
(13) J. R. Bell and D. L. Wertz, *J. Inorg. Nucl. Chem.* **35**, 137, 861 (1973).
(14) M. L. Steele and D. L. Wertz, *Inorg. Chem.*, **16**, 1225 (1977).
(15) L. S. Smith and D. L. Wertz, *J. Am. Chem. Soc.*, **97**, 2365 (1975).
(16) M. L. Steele and D. L. Wertz, *J. Am. Chem. Soc.*, **98**, 4424 (1976).
(17) H. P. Klug and L. E. Alexander, "X-ray Diffraction Procedures for Polycrystalline and Amorphous Materials", Wiley, New York, 1974, p 361.
(18) The background was ca. 4 cpm.
(19) B. D. Cullity, "Elements of X-ray Diffraction", Addison-Wesley, Reading, MA, 1956, p 172.
(20) H. A. Levy, M. D. Danford, and A. H. Narten, Report No. 3960, Oak Ridge National Laboratory, Oak Ridge, TN, 1966.
(21) B. E. Warren, "X-ray Diffraction", Addison-Wesley, Reading MA, 1969, p 145.
(22) F. Hajdu and G. Palinkas, *Acta Crystallogr., Sect. A*, **27**, 73 (1971); **28**, 250 (1972).
(23) J. H. Konnert and J. Karle; *Acta Crystallogr., Sect. A*, **29**, 702 (1973).

0020-1669/80/1319-1652$01.00/0

Table II. ARDF's of the Aqueous Iron(III) Chloride Solutions

r	*D*(*r*)	2σ	*g*(*r*)	*r*	*D*(*r*)	2σ	*g*(*r*)
A. ARDF of the 10.4 *m* ICHH Solution[a]							
0.10	0.2	2.2	2.27	4.10	646.5	7.1	1.46
0.20	1.3	2.3	1.23	4.20	526.2	7.2	1.13
0.30	2.4	2.4	1.01	4.30	408.7	7.2	0.84
0.40	1.1	2.5	0.26	4.40	346.3	7.2	0.68
0.50	−0.7	2.7	−0.11	4.50	350.1	7.2	0.65
0.60	−2.3	3.1	−0.24	4.60	407.5	7.2	0.73
0.70	−1.9	3.5	−0.15	4.70	506.8	7.2	0.87
0.80	0.0	4.0	0.0	4.80	641.2	7.2	1.05
0.90	0.8	4.4	0.04	4.90	792.7	7.3	1.25
1.00	2.8	4.8	0.11	5.00	919.8	7.3	1.39
1.10	1.2	5.1	0.04	5.10	971.1	7.3	1.41
1.20	−1.3	5.3	−0.03	5.20	921.3	7.3	1.29
1.30	−4.4	5.6	−0.07	5.30	796.8	7.3	1.07
1.40	−3.1	5.8	−0.06	5.40	665.8	7.3	0.87
1.50	−1.2	5.9	−0.02	5.50	595.6	7.3	0.79
1.60	4.9	6.0	0.07	5.60	611.9	7.3	0.74
1.70	32.4	6.1	0.42	5.70	691.1	7.3	0.81
1.80	72.5	6.2	0.85	5.80	787.7	7.3	0.89
1.90	127.1	6.3	1.33	5.90	872.8	7.4	0.95
2.00	160.9	6.3	1.52	6.00	946.9	7.4	1.00
2.10	151.2	6.4	1.30	6.10	1022.8	7.4	1.04
2.20	108.7	6.5	0.85	6.20	1100.9	7.4	1.08
2.30	69.8	6.5	0.50	6.30	1162.3	7.4	1.11
2.40	56.4	6.6	0.37	6.40	1188.5	7.4	1.10
2.50	69.5	6.6	0.42	6.50	1184.2	7.4	1.06
2.60	101.5	6.7	0.57	6.60	1178.2	7.4	1.02
2.70	145.4	6.7	0.75	6.70	1199.2	7.4	1.01
2.80	174.3	6.8	0.84	6.80	1249.3	7.5	1.01
2.90	180.6	6.8	0.82	6.90	1301.6	7.5	1.02
3.00	239.4	6.9	1.00	7.00	1325.5	7.5	1.01
3.10	306.4	6.9	1.21	7.10	1316.6	7.5	0.99
3.20	342.9	6.9	1.27	7.20	1301.8	7.5	0.95
3.30	307.4	7.0	1.08	7.30	1314.7	7.5	0.93
3.40	210.1	7.0	0.69	7.40	1365.9	7.4	0.94
3.50	119.2	7.0	0.37	7.50	1435.8	7.4	0.97
3.60	117.7	7.1	0.34	7.60	1498.0	7.4	0.98
3.70	239.7	7.1	0.66	7.70	1548.2	7.4	0.99
3.80	439.4	7.1	1.15	7.80	1609.2	7.4	1.00
3.90	619.1	7.1	1.54	7.90	1704.2	7.4	1.02
4.00	694.2	7.1	1.64	8.00	1744.1	7.3	1.03
B. ARDF of the 14.7 *m* ICHH Solution[a]							
0.10	−0.2	3.1	−0.62	4.10	749.9	6.9	1.43
0.20	−1.2	3.2	−0.96	4.20	608.4	6.9	1.11
0.30	0.0	3.2	0.00	4.30	470.3	6.9	0.82
0.40	1.4	3.3	0.28	4.40	406.6	6.9	0.68
0.50	2.5	3.5	0.32	4.50	402.5	6.9	0.64
0.60	1.2	3.8	0.11	4.60	469.2	6.9	0.71
0.70	−1.0	4.0	−0.06	4.70	587.8	6.9	0.86
0.80	−2.6	4.5	−0.13	4.80	743.8	6.9	1.03
0.90	−2.1	4.5	−0.08	4.90	907.0	6.9	1.21
1.00	0.3	4.9	0.01	5.00	1058.2	6.9	1.36
1.10	2.4	5.2	0.06	5.10	1126.3	6.9	1.39
1.20	1.0	5.5	0.02	5.20	1049.9	7.0	1.25
1.30	−1.6	5.8	−0.03	5.30	916.3	7.0	1.05
1.40	−3.5	6.0	−0.06	5.40	795.7	7.0	0.88
1.50	−2.3	6.1	−0.03	5.50	714.1	7.0	0.76
1.60	2.1	6.3	0.03	5.60	722.2	7.0	0.74
1.70	33.7	6.4	0.37	5.70	801.6	7.0	0.79
1.80	84.1	6.5	0.83	5.80	913.7	7.0	0.87
1.90	147.1	6.5	1.31	5.90	1012.4	7.0	0.93
2.00	196.1	6.6	1.50	6.00	1098.5	7.1	0.98
2.10	185.4	6.6	1.35	6.10	1166.2	7.1	1.00
2.20	126.1	6.6	0.84	6.20	1264.0	7.1	1.06
2.30	81.6	6.7	0.50	6.30	1326.3	7.1	1.07
2.40	85.5	6.7	0.48	6.40	1386.8	7.1	1.09
2.50	108.8	6.7	0.56	6.50	1404.3	7.1	1.07
2.60	136.1	6.7	0.65	6.60	1355.9	7.2	1.00
2.70	151.6	6.7	0.68	6.70	1392.1	7.2	1.00
2.80	188.7	6.7	0.78	6.80	1436.3	7.2	1.00
2.90	196.3	6.8	0.75	6.90	1496.2	7.2	1.01
3.00	261.6	6.8	0.94	7.00	1511.1	7.2	0.99
3.10	348.8	6.8	1.17	7.10	1527.5	7.2	0.97
3.20	405.3	6.8	1.27	7.20	1469.0	7.2	0.91
3.30	365.1	6.8	1.08	7.30	1501.0	7.2	0.91
3.40	229.6	6.8	0.64	7.40	1570.9	7.2	0.92
3.50	141.4	6.8	0.37	7.50	1664.6	7.2	0.95
3.60	108.3	6.8	0.27	7.60	1740.0	7.2	0.97
3.70	271.7	6.8	0.64	7.70	1790.2	7.1	0.98
3.80	462.2	6.9	1.03	7.80	1848.2	7.1	0.98
3.90	624.4	6.9	1.32	7.90	1908.5	7.1	0.99
4.00	800.0	6.9	1.61	8.00	2024.6	7.1	1.01
C. ARDF of the 4.9 *m* AIC Solution[a]							
0.10	0.2	3.1	0.69	4.10	523.1	6.7	1.08
0.20	1.1	3.1	0.95	4.20	603.1	6.7	1.19
0.30	−0.2	3.2	−0.08	4.30	686.5	6.7	1.29
0.40	−0.4	3.3	−0.09	4.40	640.8	6.8	1.15
0.50	0.1	3.5	0.02	4.50	600.3	6.8	1.03
0.60	−1.1	3.8	−0.11	4.60	540.0	6.8	0.88
0.70	−2.3	4.1	−0.16	4.70	434.3	6.8	0.68
0.80	−3.8	4.4	−0.21	4.80	428.9	6.8	0.65
0.90	−1.7	4.7	−0.01	4.90	531.5	6.8	0.77
1.00	0.9	4.9	0.03	5.00	710.5	6.8	0.99
1.10	3.1	5.1	0.09	5.10	897.2	6.8	1.20
1.20	3.2	5.3	0.08	5.20	1005.0	6.8	1.29
1.30	2.0	5.4	0.04	5.30	975.5	6.8	1.20
1.40	0.9	5.5	0.02	5.40	826.1	6.9	0.98
1.50	−0.7	5.7	−0.01	5.50	656.8	6.9	0.75
1.60	−3.0	5.8	−0.04	5.60	590.2	6.9	0.65
1.70	−2.8	5.9	−0.03	5.70	682.5	6.9	0.73
1.80	−0.6	6.0	−0.00	5.80	878.5	6.9	0.91
1.90	7.5	6.1	0.07	5.90	1056.2	6.9	1.05
2.00	62.0	6.2	0.54	6.00	1127.2	6.9	1.09
2.10	138.2	6.3	1.09	6.10	1103.6	6.9	1.03
2.20	309.1	6.4	2.21	6.20	1070.9	6.9	0.97
2.30	371.6	6.4	2.44	6.30	1096.7	6.9	0.96
2.40	211.8	6.5	1.28	6.40	1166.6	6.9	0.99
2.50	118.2	6.5	0.66	6.50	1211.5	7.0	0.99
2.60	55.2	6.5	0.28	6.60	1194.9	7.0	0.95
2.70	31.6	7.5	0.15	6.70	1164.8	7.0	0.90
2.80	69.0	6.5	0.31	6.80	1210.7	7.0	0.91
2.90	156.4	6.5	0.65	6.90	1367.1	7.0	0.99
3.00	259.2	6.6	0.99	7.00	1563.3	7.0	1.10
3.10	344.7	6.6	1.24	7.10	1679.5	7.0	1.16
3.20	401.6	6.6	1.36	7.20	1656.7	7.0	1.14
3.30	427.4	6.6	1.36	7.30	1552.5	7.0	1.01
3.40	408.7	6.6	1.23	7.40	1485.1	7.0	0.94
3.50	336.7	6.6	0.95	7.50	1523.8	7.0	0.94
3.60	450.3	6.7	1.20	7.60	1634.3	7.0	0.98
3.70	528.1	6.7	1.34	7.70	1730.3	7.0	1.01
3.80	511.6	6.7	1.28	7.80	1769.8	7.1	1.01
3.90	399.0	6.7	0.91	7.90	1791.9	7.1	1.00
4.00	430.9	6.7	0.93	8.00	1859.1	7.1	1.00
D. ARDF of the 5.7 *m* AIC Solution[a]							
0.10	0.1	2.8	0.30	4.10	675.8	6.3	1.22
0.20	0.0	2.9	0.00	4.20	854.2	6.3	1.47
0.30	−0.3	3.0	−0.10	4.30	1024.5	6.4	1.68
0.40	−0.2	3.0	−0.04	4.40	928.8	6.4	1.46
0.50	0.6	3.0	0.07	4.50	803.7	6.4	1.20
0.60	0.5	3.1	0.04	4.60	728.5	6.4	1.04
0.70	−0.4	3.2	−0.02	4.70	689.4	6.4	0.94
0.80	−2.7	3.5	−0.13	4.80	652.2	6.4	0.86
0.90	−3.2	3.7	−0.12	4.90	741.4	6.4	0.94
1.00	−2.4	4.1	−0.07	5.00	861.6	6.4	1.04
1.10	−1.2	4.5	−0.03	5.10	1068.7	6.4	1.25
1.20	0.6	4.8	0.01	5.20	1091.6	6.4	1.22
1.30	4.9	5.0	0.09	5.30	992.5	6.4	1.07
1.40	3.3	5.3	0.05	5.40	898.6	6.4	0.93
1.50	−0.7	5.5	−0.00	5.50	752.7	6.4	0.75
1.60	−4.4	5.6	−0.05	5.60	668.4	6.5	0.65
1.70	−7.5	5.7	−0.08	5.70	600.3	6.5	0.56
1.80	−4.6	5.8	−0.04	5.80	710.8	6.5	0.64
1.90	17.0	5.9	0.14	5.90	892.9	6.5	0.78
2.00	71.6	6.0	0.52	6.00	1156.8	6.5	0.97
2.10	157.3	6.0	1.08	6.10	1154.4	6.5	0.94
2.20	353.3	6.0	2.21	6.20	1051.5	6.5	0.83
2.30	427.5	6.0	2.45	6.30	988.4	6.5	0.75
2.40	280.3	6.1	1.47	6.40	1069.3	6.5	0.79
2.50	126.3	6.1	0.61	6.50	1194.7	6.5	0.86
2.60	56.6	6.1	0.26	6.60	1201.4	6.5	0.84

Table II (*Continued*)

r	$D(r)$	2σ	$g(r)$	r	$D(r)$	2σ	$g(r)$
2.70	40.3	6.1	0.17	6.70	1183.9	6.5	0.80
2.80	72.7	6.2	0.28	6.80	1265.8	6.5	0.83
2.90	156.2	6.2	0.56	6.90	1425.5	6.4	0.91
3.00	263.8	6.2	0.89	7.00	1648.6	6.4	1.02
3.10	344.9	6.2	1.09	7.10	1758.7	6.4	1.06
3.20	394.4	6.2	1.17	7.20	1838.3	6.4	1.08
3.30	408.9	6.2	1.14	7.30	1802.2	6.4	1.03
3.40	398.7	6.3	1.05	7.40	1721.7	6.4	0.95
3.50	426.6	6.3	1.06	7.50	1689.7	6.4	0.91
3.60	510.2	6.3	1.19	7.60	1799.6	6.4	0.95
3.70	581.4	6.3	1.29	7.70	1896.5	6.4	0.97
3.80	575.1	6.3	1.21	7.80	2011.6	6.3	1.00
3.90	491.1	6.3	0.98	7.90	2069.4	6.3	1.01
4.00	499.7	6.3	0.95	8.00	2119.6	6.3	1.00

[a] Calculated with a dampening factor of $-0.005\ s^2$.

Table III. Summary of the Iron(III)-Ligand Peak in Each ARDF

A. ICHH Solutions

	10.4 *m*	14.7 *m*
P1, Å	2.03	2.04
P1 area,[a] e^2	63.6	72.7
area per Fe^{3+}, e^2	2.4×10^3	2.4×10^3
2σ for P1 area,[a] e^2	3.3	3.4
resolution uncertainty, e^2	~4.0	~4.0

B. AIC Solutions

	4.9 *m*	5.7 *m*
P1, Å	2.28	2.27
P1 area,[a] e^2	94.5	116.0
area per Fe^{3+}, e^2	3.6×10^3	3.9×10^3
2σ for P1 area,[a] e^2	3.0	3.0
resolution uncertainty, e^2	~2.0	~2.0

[a] Computer integrated to a precision of $\pm 0.1\ e^2$.

Correlation of $D(r)$ with Solute Structuring. The Fe–ligand interactions may be identified from the $D(r)$'s by

$$\text{P1area}/\chi_{Fe} = \text{area per Fe} = n_{Fe-O}K_{Fe-O} + n_{Fe-Cl}K_{Fe-Cl} \qquad (2)$$

In these relationships P1area is the area under the primary peak, n_{Fe-O} and n_{Fe-Cl} are the average number of Fe–O and Fe–Cl atom pairs per Fe^{3+}, and K_{Fe-O} and K_{Fe-Cl} are the scattering power products for these atom pairs. The scattering power products may be closely approximated by the ideal peak areas; i.e., $K_{Fe-O} \simeq 403\ e^2$ and $K_{Fe-Cl} \simeq 967\ e^2$ for these solutions. Thus, the relationship

$$\text{P1area}/\chi_{Fe} \simeq \text{area per Fe} = n_{Fe-O}(403\ e^2) + n_{Fe-Cl}(967\ e^2) \qquad (3)$$

may be utilized to evaluate n_{Fe-O} and n_{Fe-Cl} in each solution.

The location of the primary peak suggests the extent of Fe–O and Fe–Cl inner-sphere bonding but can be related to the average ligand environment of Fe^{3+} in the solutions only in a qualitative manner.

Utilization of eq 3 requires that the areas under the Fe–ligand peak(s) be accurately measured, necessitating the resolution of the Fe–ligand peak(s) from the remainder of the $D(r)$. This resolution has been accomplished by "constructing" the first peak in each $D(r)$ in such a way as to be symmetrical about its maximum (Figure 2). In each case, the resulting resolution of the primary peak is consistent with the remainder of the $D(r)$. For the AIC solutions, the primary peak is sharp, leading to an uncertainty in resolution of ca. 2 e^2. The primary peak in the $D(r)$'s of the ICHH solutions is less sharp, leading to an uncertainty of ca. 4 e^2 in resolution. Each resolved primary peak has been computer integrated to a precision of 0.1 e^2.

Within the region of the primary peak, the uncertainty (2σ) has also been integrated to a precision of 0.1 e^2.

Consequently the uncertainty in the primary peak (P1) area may be attributed to the resolution of the peak (2–4 e^2), the integration of the peak (0.1 e^2), the statistical uncertainty of the primary peak (3.0–3.4 e^2), and the integration of the statistical uncertainty (0.1 e^2).

For the ICHH solutions the uncertainty is ca. 10% of the primary peak (P1) area, while it is ca. 5% for the P1area for the AIC solutions.

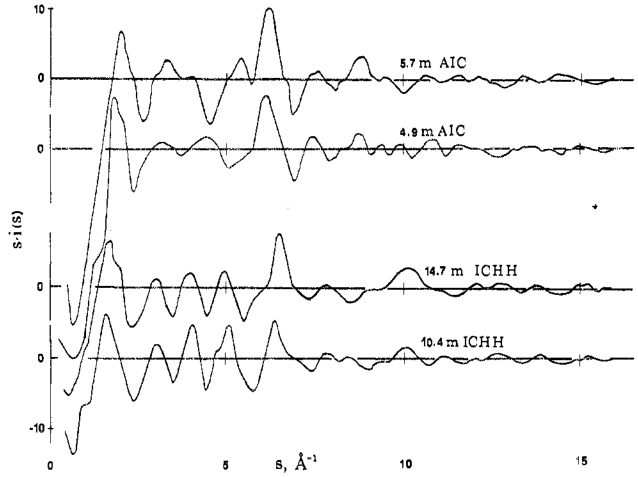

Figure 1. Unsmoothed $s[i(s)]$ curves for the four solutions. Scattering data at $s < 0.3$ Å^{-1} cannot be obtained with our θ–θ diffractometer and sample holders. The $s[i(s)]$ data were extrapolated to $s = 0.0$ by (a) assuming that $s[i(s)]$ is a smooth function in the region from $s = 0.0$ to $s = 0.5$ Å^{-1} and (b) minimizing the ripples at $r < 1.0$ Å in the resulting ARDF's.

Results and Discussion

Since the $D(r)$ of liquid water does not have a large peak in the 1.8–2.5-Å region,[24,25] the first peak in the $D(r)$ of each solution describes the average ligand environment of Fe^{3+}.

Primary Peaks. The first peak in the $D(r)$'s of the ICHH solutions is centered at 2.03–2.04 Å, and the area per Fe^{3+} is ca. 2400 e^2 for each (Table III). For the AIC solutions, the first peak, larger and sharper than the first peak in the $D(r)$'s of the ICHH solutions, is centered at 2.27–2.28 Å. The areas per Fe^{3+} are ca. 3600 e^2 for the 4.9 *m* AIC solution and ca. 3900 e^2 for the 5.7 *m* AIC solution (Table III).

The area per Fe^{3+} measured in each ARDF may be related to octahedrally or tetrahedrally coordinated Fe^{3+} by 3 and the restraints $\sum n_{Fe-O} + n_{Fe-Cl} = 4$ or 6, as shown in Table IV

The first peak in the $D(r)$ of each ICHH solution, at 2.03–2.04 Å, is consistent with the Fe–O distance found in solutions[1,2] and in crystals[26,27] where Fe^{3+} is octahedrally coordinated. Six Fe–O atom pairs [6(403 e^2)] is consistent with the area per Fe^{3+} (2400 e^2) observed for the ICHH solutions. The tetrahedral model, requiring extensive Fe–Cl bonding, may be eliminated since these $D(r)$'s do not contain a peak which may be reasonably attributed to Fe–Cl bonding. A plausible model of the solute species in the concentrated ICHH solutions is shown in Figure 3.

The first peak in the $D(r)$ of each AIC solution, at 2.27–2.28 Å, is consistent with the Fe–Cl distance found in solutions,[3] in crystals,[28-30] and in vapor-phase[31] species where Fe^{3+} is tetrahedrally coordinated. The tetrahedral model (Table IV), which requires extensive if not exclusive chloride occupation of the inner coordination sphere of Fe^{3+}, is consistent with the $D(r)$'s obtained for the AIC solutions. The octahedral model, which requires extensive Fe–O bonding, is inconsistent with each $D(r)$, since no Fe–O peak is discernible in the $D(r)$'s. In

---

(24) F. Hajdu, S. Lengyel, and G. Palinkas, *J. Appl. Crystallogr.*, **9**, 134 (1976).
(25) A. H. Narten and H. A. Levy, *J. Chem. Phys.*, **55**, 2263 (1971).
(26) N. J. Hair and J. K. Beattie, *Inorg. Chem.*, **16**, 245 (1977).
(27) M. D. Lind, *J. Chem. Phys.*, **46**, 2010 (1967); **47**, 990 (1967).
(28) B. Zaslow and R. E. Rundle, *J. Chem. Phys.*, **61**, 490 (1957).
(29) R. R. Richards and N. W. Gregory, *J. Phys. Chem.*, **69**, 239 (1965).
(30) N. C. Baenzier, *Acta Crystallogr.*, **4**, 216 (1951).
(31) E. Z. Zarison, N. G. Rambidi, and P. A. Akishiin, *Zh. Strukt. Khim.*, **4**, 910 (1963).

Table IV. Correlation of the Area per Iron(III) with Various Ligand Coordination Models

	coordination model							
	octahedral $n_{Fe-O} + n_{Fe-Cl} = 6$				tetrahedral $n_{Fe-O} + n_{Fe-Cl} = 4$			
area per Fe^{3+} from $D(r)$, e^2	n_{Fe-O}	area, e^2	n_{Fe-Cl}	area, e^2	n_{Fe-O}	area, e^2	n_{Fe-Cl}	area, e^2
		A. ICHH Solutions						
10.4 *m* soln 2400 area contribution	6.0	2410	0.0	0	2.6	1050	1.4	1350
14.7 *m* soln 2400 area contribution	6.0	2410	0.0	0	2.6	1050	1.4	1350
		B. AIC Solutions						
4.9 *m* soln 3600 area contribution	3.9	1560	2.1	2040	0.5	201	3.5	3380
5.7 *m* soln 3900 area contribution	3.4	1360	2.6	2520	0.0	0	4.0	3870

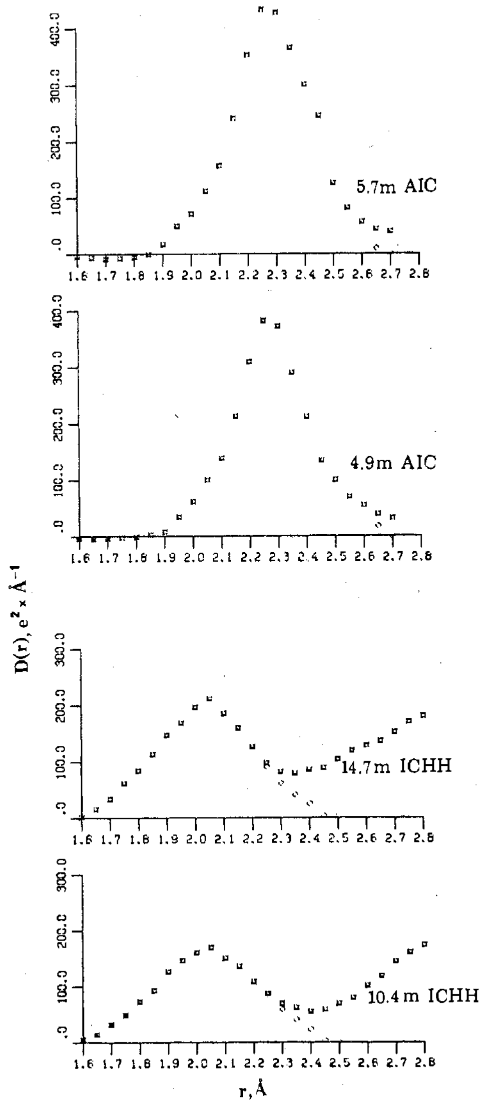

Figure 2. $D(r)$'s of the aqueous solutions prepared from $FeCl_3 \cdot 6H_2O$ and from $FeCl_3$. A plausible resolution of the first peak is shown for each $D(r)$.

the 4.9 *m* solution, the area per Fe^{3+} indicates that the average Fe^{3+} has ca. 3.5 chloride and 0.5 water neighbors, while in the 5.7 *m* solution, the average environment is ca. 4.0 chlorides and no waters. A plausible model of the solute species found in the concentrated AIC solutions is shown in Figure 4.

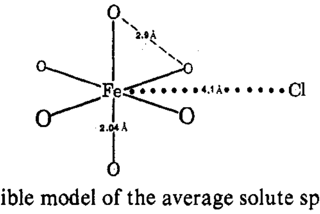

Figure 3. Plausible model of the average solute species found in the ICHH solutions.

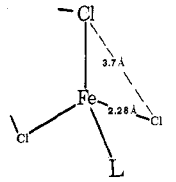

Figure 4. Plausible model of the average solute species found in the AIC solute species found in the AIC solutions. In the 4.9 *m* solution, L ≃ 0.5 chlorides and 0.5 waters. In the 5.7 *m* solution, L = 1.0 chlorides.

Hydrogen-Bonded Cl–O Peak. Each $D(r)$ contains a major peak at 3.2–3.3 Å, as do the RDF's of other aqueous solutions which contain chloride ions.[14-16,32-34] The principal, if not the exclusive, contributor to this peak is the H-bonded Cl–O interaction. Consequently, this peak cannot be utilized to validate or eliminate the various coordination models proposed above.

Ligand–Ligand Peaks. The shoulder at 2.8–2.9 Å ($2^{1/2}$(2.04 Å)) in the $D(r)$'s of the ICHH solution is consistent with the cis O···O distance in $Fe(H_2O)_6^{3+}$. A large peak at 4.1 Å (see below) is located at the expected trans O···O distance.

The large peak at 3.7–3.8 Å ($(8/3)^{1/2}$(2.28 Å)) is consistent with the Cl···Cl distance of the tetrahedrally coordinated chloroiron(III) species found in the AIC solutions.[4,28]

Ion-Pair Interactions in the ICHH Solutions. The large peak at 4.1 Å in the $D(r)$'s of the ICHH solutions is attributed to ion-pair Fe···Cl interactions. Similar ion-pair interactions have been reported.[14-16]

The $D(r)$'s of the AIC solutions do not contain a peak which may be attributed to Fe···Cl ion-pair interactions.

Solute Association in the AIC Solutions. Since $n_{Fe-Cl} > 3$ in each AIC solution, solute association via monochloro and/or dichloro bridging must occur in these solutions. While it is beyond the scope of solution XRD methods to distinguish between the monochloro- and dichloro-bridged species, the dichloro-bridged species, Fe_2Cl_6, is consistent with P3 (4.4 Å, Fe···Cl), P4 (5.2–5.3 Å, Cl···Cl), and P5 (6.0–6.1 Å, Cl···Cl). These peaks do not appear in the $D(r)$'s of the ICHH solutions.

Conclusions

Differences in the coordination details of Fe^{3+}—the average coordination number and the ligand environment—are demonstrated by the $D(r)$'s obtained for concentrated aqueous solutions of AIC and of ICHH.

The average solute species is $Fe(H_2O)_6^{3+}$ in the ICHH solutions. The Fe–O distance is ca. 2.04 Å. Chlorides occupy positions in the second coordination sphere, and the ion-pair

---

(32) J. N. Albright, *J. Chem. Phys.*, **56**, 3783 (1972).

(33) S. C. Lee and R. Kaplow, *Science*, **169**, 477 (1970).

(34) R. M. Lawrence and R. F. Kruh, *J. Chem. Phys.*, **47**, 4758 (1967).

Fe···Cl distance is ca. 4.1 Å. Cis O···O interactions are found at 2.8–2.9 Å.

In the AIC solutions, the average Fe^{3+} is pseudotetrahedrally coordinated. In the 4.9 *m* solution, the average Fe^{3+} has ca. 3.5 chloride and ca. 0.5 water nearest neighbors, while in the 5.7 *m* solution the average Fe^{3+} has 4.0 chloride nearest neighbors. The inner-sphere Fe–Cl distance is ca. 2.28 Å. The nonbonded Cl···Cl interaction, supporting the tetrahedral coordination of Fe^{3+} in the AIC solutions, is clearly discernible at $(8/3)^{1/2}(2.28\ \text{Å})$. Solute association via chloro bridging occurs in each AIC solution, and the extent of solute association is dependent upon the AIC concentration. It is beyond the scope of these solution diffraction experiments to determine if solute association leads to the dimer (Fe_2Cl_6) or to an extended solute species $(FeCl_3)_n$, although the former is more consistent with the ARDF's than is the latter.

The nearest-neighbor environments of Fe^{3+} found in crystalline $FeCl_3{\cdot}6H_2O$ and in crystalline $FeCl_3$ are retained for at least several weeks after each salt has been dissolved to prepare these concentrated aqueous solutions. The solute species initially formed in one (or both) set(s) of solutions may best be described as a kinetic product, with equilibration to the thermodynamic product being quite slow.

Registry No. $FeCl_3{\cdot}6H_2O$, 10025-77-1; $[Fe(OH_2)_6]Cl_3$, 57533-67-2; $FeCl_3$, 7705-08-0.

Contribution from the Department of Chemistry,
University of Maine, Orono, Maine 04469

Trimethylacetamide Platinum Blue

MICHEL P. LAURENT, JOHN C. TEWKSBURY, MARY-BETH KROGH-JESPERSEN,
and HOWARD PATTERSON*

Received July 12, 1979

The nature of the dichloroplatinum trimethylacetamide blue (form III) is discussed, in conjunction with results for the analogous "platinblau" and for *cis*-diammineplatinum α-pyridone blue. The methods used in this study include UV–vis spectral measurements complemented by extended Hückel molecular orbital (EHMO) calculations and Ce^{IV} redox titrations. The results suggest form III consists of a nonequilibrium mixture of oligomers of variable chain length in which there is strong Pt–Pt interaction and in which platinum is in an average formal oxidation state greater than 2. The spectral data underscore the similarity in the electronic properties of form III, platinblau, and α-PB. The EHMO calculations confirm that platinblau and form III are best not formulated as monomeric Pt^{IV} complexes.

Introduction

The so-called "platinum blues"[1] are exceptional for their intense color which contrasts with the paleness of most platinum complexes. They have also aroused particular interest because of the antitumor properties of some of the complexes without the severe nephrotoxicity of *cis*-$PtCl_2(NH_3)_2$.[1] In this report we present findings concerning the nature of platinum blues and the origin of their extraordinary color. The study was centered on the trimethylacetamide platinum blue (form III) reported by Brown et al.[2,3] Results are also presented for "platinblau"[4–6] and the recently reported *cis*-diammineplatinum α-pyridone blue[7] (α-PB). The latter is exceptional because it is, to date, the only platinum blue fully characterized structurally.

The approaches used in this investigation include the use of potentiometric titrations with Ce^{IV} to gain information on the platinum oxidation state in blues, a study of the electronic spectra of the blues as a function of medium and temperature, and interpretation of the spectral data with extended Hückel calculations.

Experimental Section

Absorption studies in the UV–vis range were made on a Cary 17 Dx spectrophotometer. Low sample temperatures were obtained with an Lt-3-110 Liquid Helium Transfer Heli-Tran.

NMR spectra were recorded on a Hitachi Perkin-Elmer R20-B spectrometer and IR spectra (4000–250 cm^{-1}) on a Perkin-Elmer PE-457 IR spectrometer. Magnetic susceptibility measurements were carried out with a Cahn Instruments Faraday magnetic susceptibility system.

Elemental analyses were performed by Galbraith Laboratories, Inc., and by Integral Microanalytical Laboratories, Inc. Molecular weights were determined by vapor-pressure depression (Galbraith Laboratories).

Syntheses. The starting materials, *cis*-$PtCl_2(NH_3)_2$[8] and *cis*-$PtCl_2(CH_3CN)_2$,[9] were prepared by the literature methods, with minor modifications.

cis-Diammineplatinum α-pyridone blue was prepared by the method of Barton et al.[7] (Anal. Calcd for $[Pt_2(NH_3)_4(C_5H_4ON)_2]_2(NO_3)_5{\cdot}H_2O$: C, 14.82; H, 2.61; N, 14.69. Found: C, 14.90; H, 2.60; N, 14.17.)

Platinblau was synthesized from *cis*-$PtCl_2(CH_3CN)_2$ as reported by Hofmann and Bugge.[4] However, the dark blue or purple powders obtained by this procedure have elemental compositions which do not

---

[1] J. P. Davidson, P. J. Faber, R. G. Fischer, Jr., S. Mansy, H. J. Peresie, B. Rosenberg, and L. Van Camp, *Cancer Chemother. Rep., Part 1*, **59**, 287 (1975).

[2] D. B. Brown, M. B. Robin, and R. D. Burbank, *J. Am. Chem. Soc.*, **90**, 5621 (1968).

[3] D. B. Brown, R. D. Burbank, and M. B. Robin, *J. Am. Chem. Soc.*, **91**, 2895 (1969).

[4] K. A. Hofmann and G. Bugge, *Ber. Dtsch. Chem. Ges.*, **41**, 312 (1908).

[5] R. D. Gillard and G. Wilkinson, *J. Chem. Soc.*, 2835 (1964).

[6] A. K. Johnson and J. D. Miller, *Inorg. Chim. Acta*, **22**, 219 (1977).

[7] J. K. Barton, H. N. Rabinowitz, D. J. Szalda, and S. J. Lippard, *J. Am. Chem. Soc.*, **99**, 2827 (1977).

[8] S. C. Dhara, *Indian J. Chem.*, **8**, 193 (1970).

[9] K. A. Hofmann and G. Bugge, *Ber. Dtsch. Chem. Ges.*, **40**, 1772 (1907).

0020-1669/80/1319-1656$01.00/0 © 1980 American Chemical Society